

# Journal Pre-proof

Collagen and chitosan blends for 3D bioprinting: A rheological and printability approach

Ana Carolina Heidenreich, Mercedes Pérez-Recalde, Ana González Wusener, Élica Beatriz Hermida



PII: S0142-9418(19)32011-2

DOI: <https://doi.org/10.1016/j.polymeresting.2019.106297>

Reference: POTE 106297

To appear in: *Polymer Testing*

Received Date: 29 October 2019

Revised Date: 6 December 2019

Accepted Date: 14 December 2019

Please cite this article as: A.C. Heidenreich, M. Pérez-Recalde, Ana.Gonzá. Wusener, É.Beatriz. Hermida, Collagen and chitosan blends for 3D bioprinting: A rheological and printability approach, *Polymer Testing* (2020), doi: <https://doi.org/10.1016/j.polymeresting.2019.106297>.

This is a PDF file of an article that has undergone enhancements after acceptance, such as the addition of a cover page and metadata, and formatting for readability, but it is not yet the definitive version of record. This version will undergo additional copyediting, typesetting and review before it is published in its final form, but we are providing this version to give early visibility of the article. Please note that, during the production process, errors may be discovered which could affect the content, and all legal disclaimers that apply to the journal pertain.

© 2019 Published by Elsevier Ltd.

## Collagen and Chitosan blends for 3D bioprinting: a rheological and printability approach

Ana Carolina Heidenreich <sup>Ψ,1</sup>, Mercedes Pérez-Recalde <sup>Ψ,1</sup>, Ana González Wusener <sup>2,3</sup> and Élica Beatriz Hermida <sup>1,3</sup>

Ψ both authors contributed equally to this work

<sup>1</sup> Lab3Bio (Laboratory of Biomaterials, Biomechanics and Bioinstrumentation), School of Science & Technology, National University of San Martín, 25 de Mayo 1143 (1650), Campus Miguelete, San Martín, Buenos Aires, Argentina.

<sup>2</sup> IIB (Biotechnological Research Institute), National University of San Martín, 25 de Mayo y Francia (1650), Campus Miguelete, San Martín, Buenos Aires, Argentina.

<sup>3</sup> National Scientific and Technical Research Council, Argentina.

\* Corresponding author: Mercedes Pérez-Recalde

Full postal address: 25 de Mayo 1143 (1650), Campus Miguelete, San Martín, Buenos Aires, Argentina

### Abstract

Collagen and chitosan are widely employed as biomaterials, including for 3D-bioprinting. However, the use of collagen and chitosan (col:chi) blends as bioinks is still scarce. In this work, the rheology of different hydrogel precursors (0.5-1.50 % w/v chi: 0.18-0.54 % w/v col) was analyzed through frequency and strain sweeps, as well as at different shear rates. Col:chi blends showed a shear-thinning behavior, with viscosity values at low shear rates between 0.35 and 2.80 Pa.s. Considering the strain rate determined by the applied flow in a 3D-bioprinter, precursor viscosities during the extrusion were in the interval 0.5-0.8 Pa.s. Printability (Pr) was measured comparing images of the printed meshes and the corresponding CAD grid design, using photograph analysis. Col:chi 0.36:1.00 was chosen to print mono-layered scaffolds for tissue engineering (TE) because of its suitable viscosity, printability and polymer ratio content. Hydrogels were obtained through NaHCO<sub>3</sub> nebulization and 37° incubation, and NHS/EDC were added to obtain scaffolds with improved mechanical behavior. They were stable after 44 h in PBS with collagenase at physiological level and showed no cytotoxic effect in NIH-3T3 fibroblasts.

**Keywords:** 3D bioprinting; hydrogel precursor rheology; collagen; chitosan; bioinks.

## 37 Introduction

38  
39 Resorbable scaffolds intend to emulate the extracellular matrix (ECM), needed for cell adhesion and  
40 proliferation, and thus for tissue regeneration. In fact, they serve as temporary constructs where cells proliferate  
41 and produce their own ECM. Methods to obtain scaffolds were profusely inquired in the literature, standing out  
42 hydrogel sponges by freeze-dry [1], hydrogels to cell delivery by injection [2] and particles for cell  
43 encapsulation [3]. Biodegradability, biocompatibility and a highly interconnected porosity are requirements for  
44 a proper performance of these scaffolds [4].

45 3D bioprinting technology is the newest technique to working with biomaterials and build wet cellular scaffolds  
46 [5]. The technique allows materials to be dispensed in a controlled, repeatable and relatively fast manner; in  
47 addition, the technique enables to add autologous cells from the patient to be treated [6]. The 3D bioprinting  
48 process involves three steps: generation of CAD file to STL of shapes to be printed - which can be set up from  
49 medical images, giving personalized scaffolds -, then biomaterials and cell dispensation, and finally printed  
50 post-processing. This last step involves crosslinking methods and the assessment of cell viability and  
51 functionality [7].

52 In 3D bioprinters, hydrogels loaded in syringes are the feeding material, accurately connected with the  
53 software design. These viscous fluids can be directly printed with cells in suspension - bioinks - or also as cell-  
54 free polymers, generating a supporting layer, alternating with cells printed from a second syringe in their  
55 culture medium, in a process called indirect bioprinting. Hydrogels have largely proved to be suitable for cell  
56 proliferation and represent a high focus research in tissue engineering. Correspondingly, hydrogels are the most  
57 used materials for 3D-bioprinting [7]. A limited variety of natural polymers are suitable for bioprinting,  
58 standing out collagen, gelatin, alginate, hyaluronic acid, chitosan, dextran and fibrin. As for other hydrogel  
59 applications, blends of them have shown improved performances, combining mechanical structure and  
60 biocompatibility [8]. Indeed, 3D bioprinting has been used to generate, for example, a heart valve with alginate  
61 and gelatin [9], myocardial tissue with alginate and RGD-modified alginates [10], a scaffold for viable  
62 hepatocytes with gelatin and chitosan [11] or nervous tissue using soybean, collagen and fibrin [12].

63 Even this background, as far as we could know there is still a lack of work regarding the use of collagen and  
64 chitosan blends as bioinks. Collagen is an animal protein extracted from connective tissues, largely used as  
65 biomaterial due to its excellent biocompatibility and availability. Type I collagen is abundant in tendons, skin  
66 and ligaments, where its fibrillar organization provides mechanical support to these tissues. Chitosan is an

67 aminated polysaccharide composed of randomly distributed monomeric units of  $\beta$ -(1-4) D-glucosamine and N-  
68 acetyl-D-glucosamine. It is a semicrystalline polymer obtained from the deacetylation of chitin, a  
69 polysaccharide mainly extracted from crustacean's exoskeleton.

70 As mentioned above, two aspects in the 3D ink development must be considered: i) features of the *hydrogel*  
71 *precursor* to achieve proper injectability and shape fidelity to the digital design, and ii) suitable mechanical  
72 properties of the *hydrogel* obtained after crosslinking, in order to allow scaffold integrity and cell proliferation.  
73 We emphasize, in this contribution, on the rheological properties and shape fidelity - *printability* - of the  
74 *hydrogel precursors* containing different proportions of chitosan and collagen.

75 Both collagen and chitosan were reported as exhibiting pseudo-thinning behavior in diluted solutions [13].

76 Thus, viscosity in the shear rates at applied stresses during the extrusion becomes relevant since it influences  
77 printing accuracy. In these sense, a suitable viscosity range for extruding is between 0.30 and 30 Pa.s, since  
78 higher values bring large pressure to hydrogel extrusion out of the nozzle, and the process becomes unstable  
79 [14].

80 Printability (Pr), is affected not only by ink features but also by process parameters such as extruder head speed,  
81 ejected material volume, extrusion nozzle size and distance between nozzle and substrate. Several studies relate  
82 printing parameters to the process results by measurements methods, even if it doesn't exist an only way to  
83 determine Pr. One method, for instance, is by printing grids and relating the hole designed area in the grid to the  
84 real area obtained by printing; another method is by printing sharp angles and assessing overlap between lines  
85 [14]. In other cases, also working with meshes and designed squared holes, Pr can be determined by measuring  
86 the circularity of the closed area and the perimeter of the printed square [15].

87 After printing, the pathway from hydrogel precursor to hydrogel is given by intermolecular forces among the  
88 polymer chains. For chitosan, pH neutralization is enough to trigger gelation process; in the case of collagen,  
89 pH neutralization and temperature, commonly 37°, is required. In addition, to obtain stronger gels, cross-linking  
90 agents such as genipin [16] [17] glutaraldehyde [18] [19], NHS and EDC/EDAC [20] are widely employed, as  
91 promoters of covalent links between chains. Finally, the swelling or contraction features in physiological  
92 medium are considered so that the deformation of the final construct can be minimized.

93 Collagen and chitosan blends are very well characterized as biomaterials with excellent features in tissue  
94 engineering; studies have strongly focused in dry scaffolds, sponges [1] [19] [20] or microspheres [21] as well  
95 as dry scaffolds including hyaluronic acid in triple blends [22][23]. However, the study of these blend  
96 properties as viscous fluid, is less explored. A thermal and rheological study for a blend 1:1 ratio col:chi, has  
97 been carried out, performing frequency sweeps, and apparent viscosity determinations, in which blends

98 viscosities values ( $\sim 1$ - $0.1$  Pa.s) at different shear rates were between collagen alone ( $\sim 10$ - $0.2$  Pa.s) and  
99 chitosan alone ( $\sim 0.01$ - $0.006$  Pa.s), both three with shear thinning behavior [13]. In another study, col:chi at five  
100 different ratios from 1:1 to 50:1 were assessed about injectability as hydrogels carrying endothelial cells,  
101 determining the onset of gelation measured as a time-dependent change in viscosity [24]. Reis and coworkers  
102 [2] studied col:chi hydrogels with a peptide-modified chitosan, assessing different ratios in final concentrations  
103 between 0.25 and 0.50 % w/v, performing rheological assays, cardiomyocytes culture *in vitro* and animal  
104 injections with. In another study, col:chi hydrogels with bioactive glass nanoparticles for injectable systems  
105 were assessed, using chi 2 % w/v and col 0.20 % w/v in a 70:30 ratio and performing rheological assays to  
106 evaluate gel formation at different temperatures [3].

107 Col:chi blends as inks for 3D bioprinting are still poorly characterized. Indeed, Murphy and coworkers [25]  
108 assessed twelve different hydrogels for bioprinting for skin regeneration, one of which was col:chi 0.1%  
109 w/v:1.5% w/v. The study comprised cell viability, degradation and gelation; however, rheological studies were  
110 not part of this work, neither printability for the chosen col:chi blend. Taking into account the chitosan and  
111 collagen features and the wide bibliography about col:chi scaffolds for tissue engineering, the aim of this work  
112 is to study rheological features and printability of col:chi blends, seeking for proper inks for extrusion 3D  
113 bioprinting.

## 114 **Materials and Methods**

### 115 **Collagen Extraction**

116 The extraction protocol was made according adaptations of previous works [26][27]. Briefly, fresh tails were  
117 placed in 96% ethanol and incubated at  $-20^{\circ}$  for at least 24 hours. The skin was removed, exposing the white  
118 tendons, in which their composition is approximately 80-90% collagen fibers. Tendons were detached with a  
119 clamp and placed in sterile PBS. Exposed fibers were cut into portions of approximately 1 cm long and were  
120 placed in 1:1000 glacial acetic acid, at a volume of 50 ml per tail. They were left under magnetic stirring at  $4^{\circ}$   
121 during 48 h. A first centrifugation was made at  $1000\times g$  for 20 minutes at  $4^{\circ}$  and supernatant was recovered. A  
122 second centrifugation was carried out for 15 min at  $10000\times g$  at  $4^{\circ}$ , also obtaining the supernatant: a very  
123 viscous solution. 2 ml aliquot, by triplicate, was freeze-dried and weighted to know collagen concentration.  
124 Fresh collagen was usually used; the rest of solution was freeze-dried and resuspended in 1:1000 acetic acid to  
125 obtain desired concentrations. Extraction protocol was repeated three times with similar results. Collagen fibers  
126 and fibrils were observed with an Atomic Force Microscope (Supplementary Data Fig. 1).

### 127 **Collagen:Chitosan (col:chi) Inks**

128 Low molecular weight powder chitosan (Sigma-Aldrich: deacetylation degree 92% and viscosity 46 cps for the  
 129 1% solution) was employed to preparing solutions. 0.10 M acetic acid was used as a solvent to achieve a 2 %  
 130 w/v solution by magnetic stirring at room temperature. Final pH was ~4.50. Col:chi blends were obtained from  
 131 different volumes of chi 2 % w/v and col 0.72 % w/v stock preparations, to obtain, in % w/v: col:chi 0.36:0.50;  
 132 col:chi 0.54:0.50; col:chi 0.24:1.0; col:chi 0.36:1.0; col:chi 0.18:1.5 and col:chi 0.45:1.5. Final blends had  
 133 pH=4.50 and showed excellent miscibility. All of them were used as hydrogel precursors – inks – and stored at  
 134 4°.

### 136 **3D-Bioprinter**

137 A low-cost bioprinter (3-DonorRes, trademark LIFE SI, Argentina) with two syringes, one of them  
 138 thermostated, was used for printing. Software parameters allowed to control ejection time, material amount in  
 139 each dot, and the distance between dots; two first parameters were changed in Printability assays in order to  
 140 obtain different flows. In all cases, a 25G needle was used and the distance between needle and bed was  
 141 approximately 1 mm. Temperature during extrusion process was room temperature, both in ejection chamber  
 142 and in at deposit bed.

### 144 **Flow estimation**

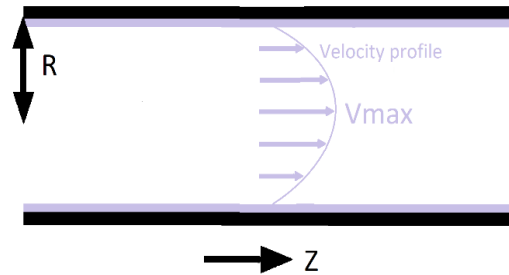
145 Strain  $\gamma$  imposed by syringe piston during the extrusion process was estimated according to the equation 2,  
 146 where  $\Delta z$  represents the lengthwise displacement, and R the needle radio (Fig. 1). This simplification is  
 147 possible because the Reynold's number is under 2000, which is the limit where a laminar flux may be  
 148 supposed.

$$\gamma = (\Delta z/R) \quad (eq.1)$$

149 So, strain rate was obtained as the derivative with respect to time, as it is expressed in eq. 3.

$$\dot{\gamma} = 1/R \Delta z/\Delta t \quad (eq.2)$$

150



151

152 **Figure 1:** Schematic lumen needle with radio R and distance Z. Laminar flux approach is considered due to Reynold's number under  
 153 transitional level to turbulence. Adapted from Amer et al [28].

154 Displaced volume  $\Delta V$  in the cylindrical geometry of the lumen is related with  $\Delta z$  as indicated with equation 3.

$$\Delta V = \pi R^2 \Delta z \text{ (eq. 3)}$$

155 By combining equations 3 and 4, shear rate and flow  $\left(\frac{\Delta V}{\Delta t}\right)$  are related according with equation 4.

$$\dot{\gamma} = 1/(\pi R^3) \Delta V / \Delta t \text{ (eq. 4)}$$

## 156 Rheology

157 A rheometer TA Discovery Hybrid HR-3 was used, with a 40 mm diameter 2-degree cone plate geometry, a  
 158 truncation gap of 60  $\mu\text{m}$  and a solvent trap to prevent drying. Only when total polymer concentration was under  
 159 1.00 % w/v concentric cylinders geometry was used. Storage modulus ( $G'$ ) and loss modulus ( $G''$ ) were  
 160 recorded as a function of strain [0.25- 450] % at constant frequency 1 rad/s (oscillatory mode). Frequency  
 161 sweeps [0.15-10] rad/s at constant strain amplitude 1% (oscillatory mode) was performed to obtain the storage  
 162 modulus ( $G'$ ), loss modulus ( $G''$ ) and complex viscosity ( $\eta^*$ ). Apparent viscosities were measured as a function  
 163 of the shear rate  $\dot{\gamma}$  [0,015-100] $\text{s}^{-1}$  (flow mode). All experiments were made at 25° and at least by duplicate.  
 164 TRIOS software in the rheometer was used to fit zero rate viscosity with the best model.

## 165 pH neutralization and gelation

166 Immediately after printing,  $\text{NaHCO}_3$  0.80 M nebulization was made to neutralize the scaffolds. A San-Up  
 167 Model 3042/3059 ultrasonic nebulizer was used, which provided drops with diameters between 1.5 and 5.7  $\mu\text{m}$ ,  
 168 at an oscillation frequency of 2.5 MHz and a flow rate of at least 0.5ml / min. Three 5-minutes cycles were  
 169 performed, controlling the pH increase after each nebulization cycle with pH paper, until pH ~7.50 was

reached; the last control of pH was performed with a pHmeter. Then, nebulized scaffolds were incubated at 37°  
in a water bath during 30 minutes.

### **Crosslinkers addition before printing**

EDC (1-ethyl-3- (3-dimethyl aminopropyl) carbodiimide) and NHS (N-hydroxysuccinimide), both from Termofisher, were added in powder form into the hydrogel precursor solutions, until 15 mM and 6 mM were achieved, respectively. The crosslinked col:chi mix was vortexed and kept at 0 °C until loaded into the syringe until printing. Subsequently, to achieve the hydrogel the protocol was the same as in the previous section, but with a 10 minutes nebulization cycle and a 5-minutes stabilization.

### **Mechanical properties**

1mm thickness and 12 mm diameter round-trip samples were printed. A dynamic mechanical analyzer (DMA) model Q800 was used (TA Instruments, DE, USA) to determine their mechanical response. Compression tests were performed on the substrates using the 12 mm diameter geometry, in controlled force mode, at 37 °. The preload force was 0,01 N, the force ramp 0,02 N/min and the force limit 1N. The compression modulus (E) was calculated as the slope value in the linear section of the curve "tension vs. deformation" between 5 % to 10 % of deformation (n=3).

### **Printability**

To measure Printability (Pr), a mesh with square holes of 4 mm on each side was chosen (Fig. 2). The strand thickness was 0.3 mm so that the software that commanding the printer, slic3r, generates in the GCODE a single path of the extrusion head per side. The design was made with CAD software. Three different printing conditions - 1, 2, 3 - were assayed taking advantage of the software possibilities, varying speed and material amount, so that flows were 0.19 µL/s, 0.42 µL/s and 0.35 µL/s, respectively.

Pr index by area compares printed area versus those in digital design [6] [7], according to the equation 5, where nearer to 1, better the printing fidelity.

$$Pr = A/A_{theoretical} \quad (eq. 5)$$



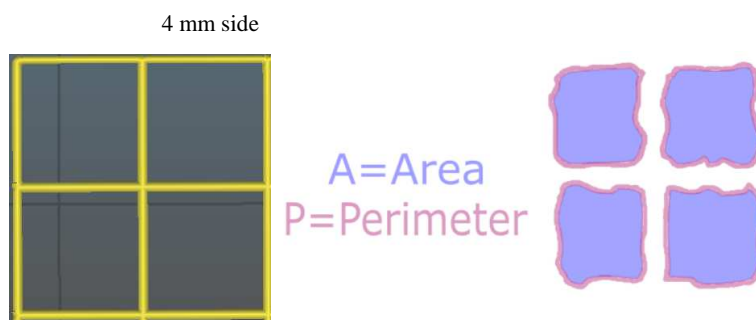


**Figure 2:** Digital model and parameters measured in each hole from printed grids

$A$  is the printed area, determined by images and the Image-J®, and  $A_{theoretical}$  is the grid area according to the design.  $P$  refers to the printed square perimeter and  $A$  is the measured area. To construct the meshes, hydrogel precursors were loaded in a 1 ml syringe. A glass slide with a 1-2 mm thickness was used as support for the mesh. Images were acquired immediately after printed. At least 24 squares were measured in order to determine  $A$  mean values.

### Stability in PBS and in PBS/collagenase.

15mm x 15mm x 1mm height square geometries were printed with approximately 250  $\mu$ l of ink ( $n = 5$ ). Samples were weighed to determine their initial weight,  $W_0$ , and were immersed in PBS pH=7.4, at 37° during 72 h. Scaffold weight was controlled each day, extracting them from the solution and drying them by draining by gravity, supporting the scaffolds with a piece of paper. Residual mass (M.R.) was calculated as the ratio between the weight of the dry substrate at a time  $t$  ( $W_t$ ) and the mass of the initial test piece ( $W_0$ ), as  $M.R. (\%) = W_t/W_0 * 100\%$

In parallel, a solution of PBS pH 7.4 was prepared including 60  $\mu$ l of 1mg /ml collagenase solution (from *Clostridium histolyticum*, Sigma) each 5 ml of PBS. Samples ( $n=5$ ) obtained as in the paragraph above, were immersed in 4 ml of collagenase/PBS solution. Two test pieces were used as positive control, printed by the same way but containing only collagen 0.72% w/v. They were incubated at 37° for 48 h, or until their complete breakup in the case of positive controls. Each sample weight was taken at different times after being drained by gravity and by blotting paper. The residual mass percentage was calculated by the M. R. % equation.

### Scaffolds Cytotoxicity

**Direct Toxicity.** NIH/3T3 cells were incubated in direct contact with the col:chi scaffolds.  $1.10^5$  cells were incubated in a 24-well plate (Corning Costar, MA) at 37° for 24 h in a 5% CO<sub>2</sub> humidified incubator. Samples

218 and control materials were put in each well, occupying 10 % of the well area. Complete culture medium was  
219 used as null control. As a positive control, we used latex rubber. Teflon (DuPont, DE) was used as a negative  
220 control, since it has no known *in vitro* cytotoxic effects. Cells were incubated in contact with the samples for 24  
221 h at 37° in a 5% CO<sub>2</sub> humidified incubator. The cytotoxicity was assessed qualitatively. Cells were examined  
222 microscopically in a Nikon TE2000-U inverted microscope coupled to an ORCA-ER CCD camera  
223 (Hamamatsu). Changes in general morphology, vacuolization, detachment and cell lysis were assessed. All  
224 experiments were performed in triplicate.

225 **Indirect Cytotoxicity.** Material extracts were prepared by incubating scaffolds and control samples in complete  
226 medium with a material area (cm<sup>2</sup>): media (ml) ratio of 6:1, for 72 h at 37° in a humidified atmosphere  
227 containing 5% CO<sub>2</sub>. Scaffolds extracts were compared with medium control, positive control (latex rubber)  
228 extract and positive negative control (Teflon, DuPont, DE). 1.10<sup>5</sup> NIH/3T3 cells were incubated in a 24-well  
229 plate (Corning Costar, MA) at 37° in a 5% CO<sub>2</sub> humidified incubator. After 24 hours of incubation, the culture  
230 medium was replaced for the pure extract or 1/16 dilution of the extract in complete medium. Cells were  
231 incubated with the extracts for 24 h. Cells were examined microscopically in a Nikon TE2000-U inverted  
232 microscope coupled to an ORCA-ER CCD camera (Hamamatsu). Changes in general morphology,  
233 vacuolization, detachment and cell lysis were assessed. All tests were performed by triplicate.

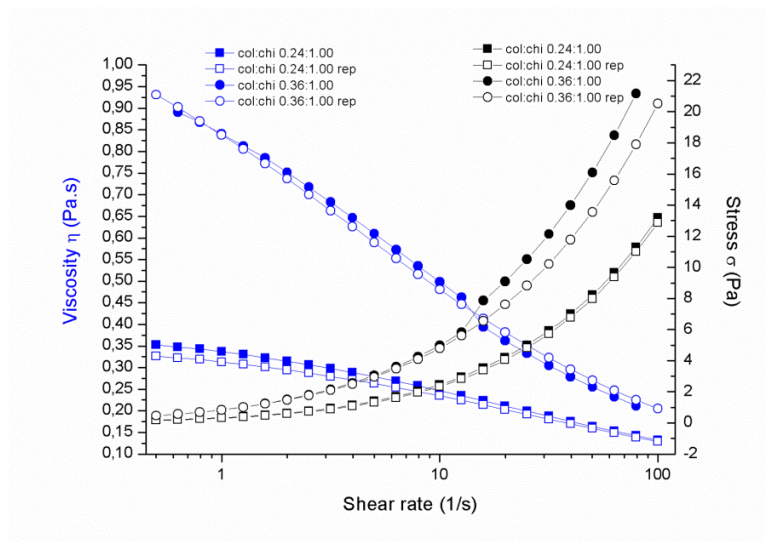
## 234 Results and Discussion

### 235 1. Rheology of the inks

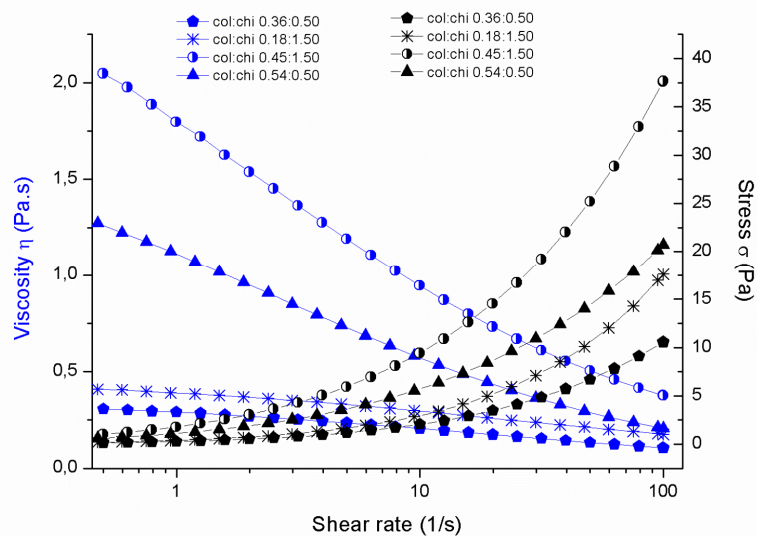
236

237 Rheological analysis to six col:chi hydrogel precursors were performed, under rotational mode (Fig. 3) and  
238 under oscillatory mode (Fig. 4 and 5). Apparent viscosity ( $\eta_{app}$ ) and corresponding stress ( $\sigma$ ) under different  
239 shear rates (0.50 to 100 1/s) are presented in Fig. 3. Shear-thinning behavior was evident for all blends, as  
240 viscosities decreased with the shear rate. In Fig. 3.a, two inks with the same chitosan concentration (1.00 %  
241 w/v) but differing in collagen content (0.24 and 0.36 % w/v) are presented, with their duplicates. As reported  
242 previously in col:chi blends rheological analysis [13], collagen component strongly contributes to the viscosity.  
243 Zero rate viscosities were  $0.383 \pm 0.01$  Pa.s (col:chi 0.24:1.00) and  $1.16 \pm 0.08$  Pa.s (col:chi 0.36:1.00)  
244 according to our data and to Carreau-Yasuda model. In Figure 3.b, viscosity curves from four blends containing  
245 chitosan 0.50 % w/v (col:chi 0.36:0.50 and col:chi 0.54:050) or 1.50 % w/v (col:chi 0.18:1.50 and col:chi

246 0.45:1.50) are presented, in this case one representative sweep of each blend. They exhibited similar behavior  
 247 than both chitosan 1.00 % w/v inks regarding shear- thinning behavior as well as collagen viscosity influence.  
 248 Beyond the total polymer concentration, collagen influence may be appreciated, for instance, comparing col:chi  
 249 0.54:0.50 with higher viscosity curves by comparison with of col:chi 0.18:1.50.

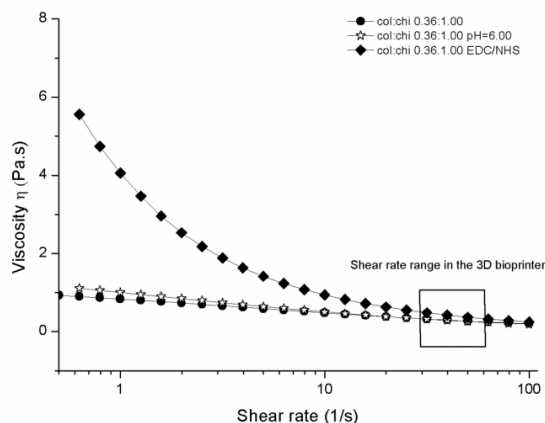


(a)



(b)

254



255

256

(c)

257

258

259

260

**Figure 3:** Apparent Viscosity as a function of shear rate (a) for two pH=4.50 col:chi blends sharing chitosan composition 1% w/v; (b) for four pH=4.50 col:chi blends, with chitosan 0.50 % w/v or with 1.50 % w/v; for clarity one replicate is shown, and (c) for col:chi 0.36:1.00 in comparison with the same ink after adding in crosslinkers (col:chi 0.36:1.00 EDC/NHS) and after raising its pH to 6.00 (col:chi 0.36:100, pH=6.00).

261

262

263

264

265

266

267

268

269

270

271

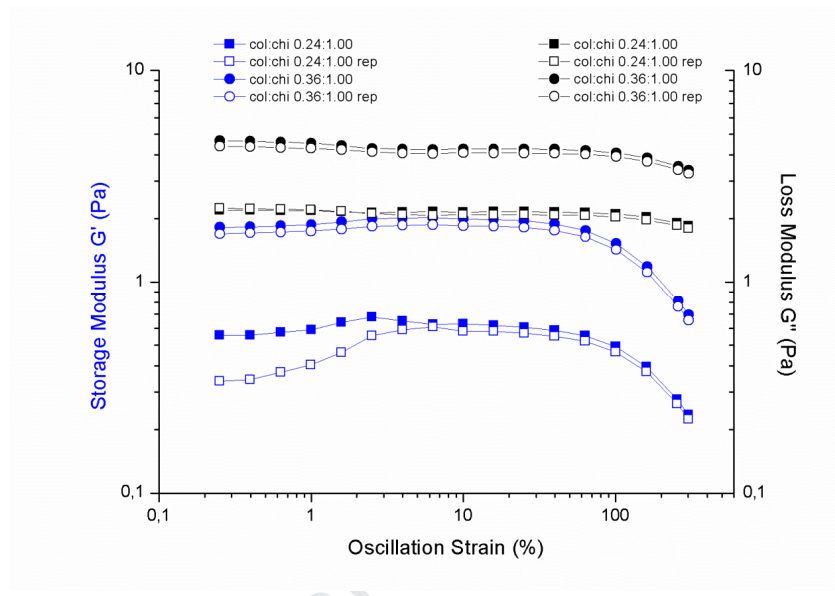
In Fig. 3.c, a comparison between one selected ink (col:chi 0:36:1.00) and its viscosity behavior at pH=6.00 is shown. Considering the possibility of direct bioprinting, hydrogel precursor pH increase becomes necessary: the results indicated that viscosity increased at low shear rates (zero rate viscosity col:chi 0.36:1.00 pH=6.00 2.50 Pa.s) and was almost non variable values at shear rates upper than 40 (1/s). Similar results were obtained with col:chi 0.54:0.50 at pH=6.00 (data not shown). In addition, col:chi 0.36:1.00 including NHS and EDC crosslinking activators is showed in 3.c. In this case, viscosity increase was considerable and the difference with the original ink started decreasing since 20 (1/s). As it was introduced above, viscosity in the shear rates at applied stresses during the extrusion becomes relevant as influences printing accuracy. Fig. 3.c shows the working range shear stress - 30-60 (1/s) - with the 3D bioprinter that will be exposed in Section 2 of Results. Ink treatment with NHS/EDC to improve printed scaffold final mechanical properties will be discussed in Section 3 of Results.

272

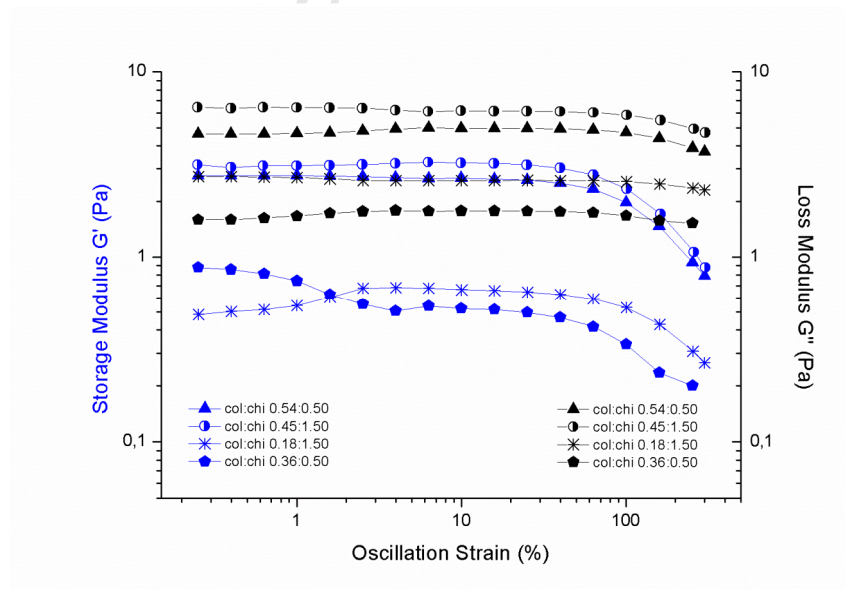
273

Although low-viscosity precursors are important for cell viability in a direct printing approach, some authors emphasize about the importance of high viscosities to improve printing process [29] suggesting the viscosity

274 modulation using pre-crosslinking methods; e.g., to partially crosslink increasing viscosity at the hydrogel  
 275 precursor state. Several works have used this approach typically with calcium to alginate. In our case, a pre-  
 276 crosslink by pH increase, was observed in Fig. 3.c. In the same way, a higher effect was observed on the  
 277 viscosity by adding NHS/EDC crosslinkers into this precursor stage.



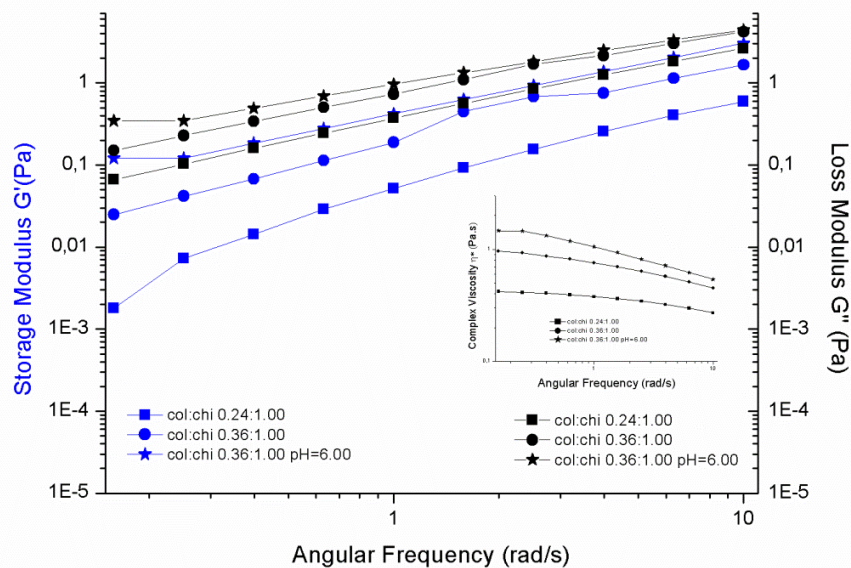
(a)



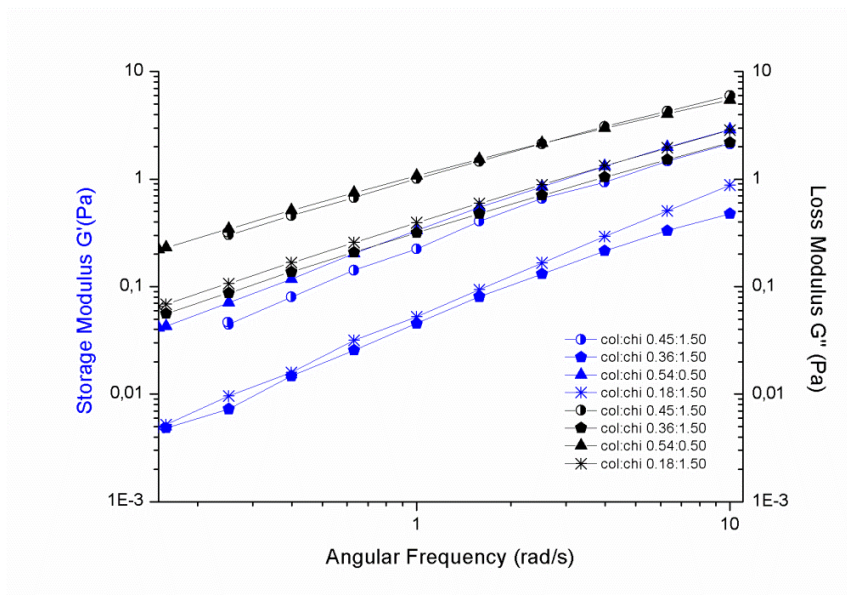
(b)

281 **Figure 4:** Storage Modulus ( $G'$ ) in blue and Loss Modulus ( $G''$ ) in black as a function of the oscillation strain (a) for two pH= 4.50  
 282 col:chi blends sharing chitosan composition 1% w/v, by duplicate and (b) for four pH=4.50 col:chi blends, with chitosan 0.50 % w/v  
 283 or with 1.50 % w/v; for clarity one replicate is shown.

284 In Fig. 4,  $G'$  and  $G''$  from amplitude sweeps of the six col:chi blends are shown. Linear viscoelastic range  
 285 (LVR) could be observed in  $G'$  curve, showing linearity between 5 and 80 % of oscillation strain. Both Fig. 4.a  
 286 and 4.b graphs exhibit materials with viscous component more important than solid component, according with  
 287 these low-viscosity hydrogel precursors.



(a)



(b)

**Figure 5:** (a) Loss modulus ( $G''$ ) in black, storage modulus ( $G'$ ) in blue and complex viscosity ( $\eta^*$ ) in the inset as a function of the frequency for two pH=4.50 col:chi blends sharing chitosan composition 1% w/v and col:chi 0.36:1.00 at pH=6. (b) Loss modulus ( $G''$ ) in black and storage modulus ( $G'$ ) in blue as a function of the frequency for four pH=4.50 col:chi blends, with chitosan 0.50% w/v or 1.50% w/v. For clarity in the graphs only one representative sweep of each ink is shown.

In Fig. 5, frequency sweeps show that in all cases the loss modulus ( $G''$ ) was higher than the storage modulus, prevailing the viscous-like behavior in these viscoelastic fluids. pH=6.00 ink in (a) exhibited similar behavior than the original at pH=4.50, but with higher values. Since no crossover between modulus, all of the inks show stability at  $25^\circ$  under these conditions.

In bioinks research, it is known that shear thinning performance contributes positively to 3D bioprinting, being advantageous for print fidelity and also for cell protection. Shear thinning performance enables a decreasing proportional stress with increasing flow that results in less stress for the cells [29]. Yield stress and recovery time are another interesting aspects to considering when bioinks rheology is deepened [30].

## 2. Printability

Using eq. 4 from Methods, the shear rate applied to the ink at three different conditions in the 3D bioprinter, has been estimated. Table 1 presents the shear rates values, for a 25 G needle (260  $\mu\text{m}$  internal diameter) at the flow imposed in each condition. Even if Printability is usually described as dependent of the hydrogel viscosity [31], it is important to note that for the same ink by different set conditions, e.g. different flow rates, viscosity and printing quality may change. In addition, the high pressure and small nozzle diameters represent possible damages to cells. Material amount and printing speed determine the line width of the construct [31]. Although, low pressures and bigger sized nozzle may be favorable for cell viability after printing, but it can result in a structure with low shape fidelity. So, the advantages and drawback are important to select printing conditions. By last, at one determined condition the needle tip to bed printing distance may influence the final quality; in this work prints were always performed at the constant distance of about 1 mm.

Printing Condition	Flow [ul/s]	Shear rate[1/s]
1	$0,19 \pm 0,09$	$30 \pm 10$
2	$0,42 \pm 0,04$	$62 \pm 7$
3	$0,35 \pm 0,07$	$50 \pm 10$

**Table 1.** Estimated shear rates for the flows at the working conditions in the 3D-bioprinter, fed with different col:chi inks.

Three inks printability in conditions 1, 2 and 3 were analyzed. Inks were chosen so that they represent the variety regarding polymer contents while those with lowest viscosity were discarded. So, col:chi 0.54:0.50, col:chi 0.36:1.00 and col:chi 0.18:1.5 were selected. In addition, thinking in a future bioink and taking into account the low pH of all these blends, col:chi 0.36:1.00 was used to generate a new hydrogel precursor (col:chi 0.36:1.00 pH ~ 6.00) by carefully adding NaOH 1.00 M drops with fast and enough vortexing. Given that the ratio 1:1 was quite explored in the scaffolds literature, col:chi 0.36:1.00 was selected because its good rheological features (always nearby to col:chi 0.54:0.50, in viscosity above all at the 3D printer shear rates) and because the possibility of more physiologically stable scaffolds – more chitosan content – [1].

From image analysis and according to eq. (6) from Methods, Pr values were obtained (Table 2). Pr as representing a measure about some material tendency to dilatate or to flux, in the case of this design reducing the hole area. In our inks, we could appreciate that the higher the flow - the lowest viscosity during the



extrusion - the worst performance in Pr measurements. These observations were in agreement with the fact that too low viscosities do not allow to maintain the shape in relation to the digital design (see below Fig 6.b).

Ink (col:chi)	Shear rate $30 \text{ s}^{-1}$ Flow $0.19 \text{ } \mu\text{L}/\text{seg}$ (PC 1)	Shear rate $62 \text{ s}^{-1}$ Flow $0.42 \text{ } \mu\text{L}/\text{seg}$ (PC 2)	Shear rate $50 \text{ s}^{-1}$ Flow $0.35 \text{ } \mu\text{L}/\text{seg}$ (PC 3)
	Pr	Pr	Pr
0.54:0.50 $\text{pH}=4.50$	$0.67 \pm 0.11$	$0.68 \pm 0.13$	$0.75 \pm 0.12$
0.36:1.00 $\text{pH}=4.50$	$0.74 \pm 0.20$	$0.49 \pm 0.18$	$0.67 \pm 0.13$
0.36:1.00 $\text{pH}=6.00$	$0.69 \pm 0.12$	$0.72 \pm 0.15$	$0.68 \pm 0.19$
0.18:1.50 $\text{pH}=4.50$	$0.69 \pm 0.18$	$0.56 \pm 0.18$	$0.72 \pm 0.15$

**Table 2.** Printability values assessed by square area (Pr) under three different printing conditions (PC) with determined flows and associated shear rates, for four different hydrogel precursors (inks) made with collagen (col) and chitosan (chi).

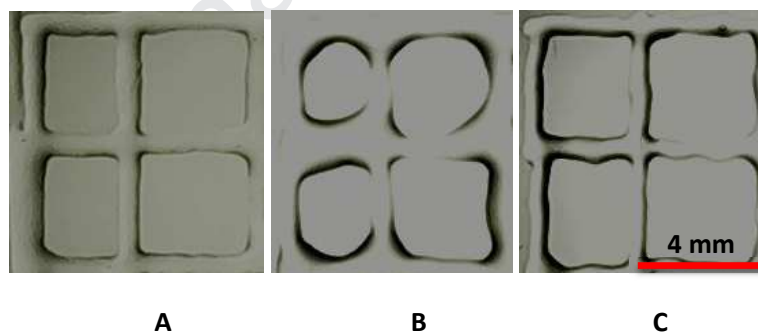


**Figure 6.** Printed grids with col:chi 0.36:1.00 ink, under conditions 1 (A, flow  $0.19 \text{ } \mu\text{L}/\text{s}$ ; shear rate  $30/\text{s}$ ), 2 (B, flow  $42 \text{ } \mu\text{L}/\text{s}$ ; shear rate  $60/\text{s}$ ) and 3 (C, flow  $0.35 \text{ } \mu\text{L}/\text{s}$ ; shear rate  $50/\text{s}$ ).

Fig. 6 shows printed grids representative pictures under each printing condition, using col:chi 0.36:1.00 ink. Condition 1 (Fig 6.A), is associated with the lowest flow ( $0.19 \text{ } \mu\text{L}/\text{s}$ ) given that its low ejection speed and a small material amount: this condition seemed to enable the better results, also quantified by Pr index in Table 2. Under condition 2 (Fig 6.B), a filament thickness effect was observed, probably due to a high material amount

351 needed to achieve the flow  $0.42 \mu\text{L/s}$ , resulting in poor shape fidelity. Finally, in Fig 6.C results of printing  
352 condition 3 is observed; in this case, the flow  $0.35 \mu\text{L/s}$  was reached increasing the ejection speed relating to  
353 printing conditions 1. A slight line undulation evidenced the higher speed and influenced negatively the printing  
354 quality. Depending of the future use of printed forms, these observations could be important if small or linear  
355 geometries are required. However, they could be less important in big printed areas (e.g. wound patches), where  
356 probably the insuming time becomes a more critical variable. For the first case, results under the PC 1 and PC 3  
357 seem to be independent from inks viscosities in the range here used ( $0.50\text{-}1.80 \text{ Pa}\cdot\text{s}$ ), showing similar Pr values  
358 among inks. Conversely, with the higher flow (PC 2), only inks in the higher range of viscosity values showed  
359 acceptable performance, exhibiting their capacity of holding the size without spreading. In this sense, even if  
360 the pH increase to the chosen ink col:chi 0.36:1.00 had null effect under PC 1 and PC 3, it had some positive  
361 impact according in PC 2, probably because of a viscosity change. According to rheological determinations, for  
362 the pH=6.00 ink similar features to the original blend (pH=4.50) were found but greater  $G'$  and smaller  $G''$ .

363 As it was mentioned above, regarding Pr some authors emphasize the pre-crosslinking approach to improve the  
364 shape quality, instead of a change in polymer concentration affecting cells. So, to be able to regulate viscosity  
365 and shape quality, for example by calcium ions or temperature, in the profusely studied alginate/gelatine ink,  
366 for example [15] [29].

### 368 **3. Substrate for Tissue Engineering**

369  
370 Squares of  $1 \text{ cm} \times 1 \text{ cm} \times 1 \text{ mm}$  thickness were printed with the selected col:chi 0.36:1.00 ink. Triggering the  
371 gelation through  $\text{NaHCO}_3$  nebulization and  $37^\circ$  incubation, we observed a resulting homogenous hydrogel but  
372 fragile and deformable substrates were obtained. This same feature have shown scaffolds obtained from other  
373 assayed inks as col:chi 0.54:0.50. Given that, NHS/EDC crosslinkers activators were added to the hydrogel  
374 precursors in solid form just before printing. These two agents covalently link carboxyl or phosphate groups to  
375 primary amines giving covalent unions amide both between collagen-collagen and between collagen-chitosan.  
376 According to the literature, this treatment appears always by immersion in NHS/EDC solutions [20] [32], and  
377 as far as we know it is the first report under this approach.

378 After printing and gelation, obtained substrates had suitable manipulable features (Fig. 7) and their elastic  
379 modulus E was estimated as  $1.95 \pm 0.14$ .

Even if the printing quality and performance in the syringe were accurate, when we analysed the precursor col:chi 0.36:1.00<sub>EDC/NHS</sub> by rheological properties, an increase in the ink viscosity ( $\eta_{app}$ ) was detected, in comparison with the original ink (see Fig. 3.c). Associated values with shear rates in printing conditions 1, 2 and 3 were 0.52 Pa.s, 0.34 Pa.s and 0.37 Pa.s, respectively, in comparison with 0.35 Pa.s, 0.25 Pa.s, 0.27 Pa.s for the original col:chi 0.36:1.00. Measurements were made immediately after adding the crosslinkers, and during approximately 40 minutes. We noticed a strong tendency to viscosity increase at room temperature, so that keeping on ice was always necessary after the crosslinker addition. Time sweeps at 0° in rheometer have confirmed that at least during 40 minutes gelation does not occur, even if  $G'$  approaches to  $G''$  (See Fig.1 Supplementary Data).

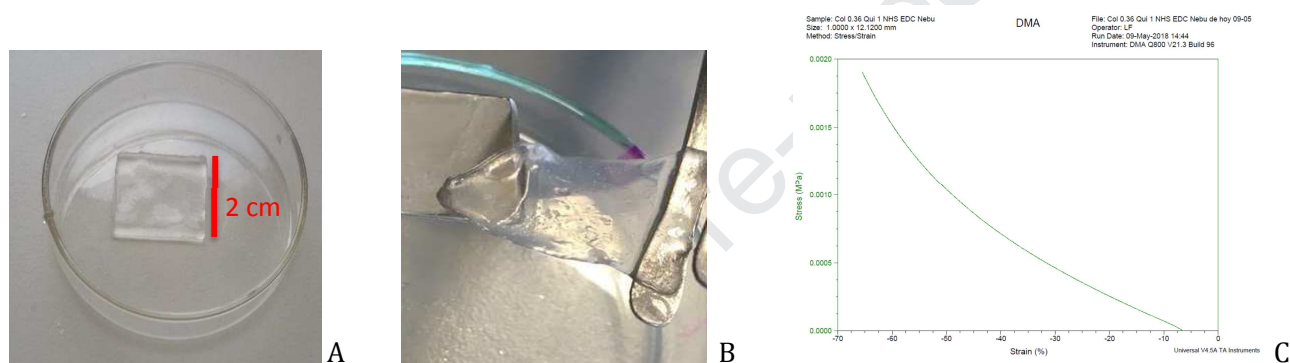


**Figure 7.** Example of mono-layered substrate from col:chi 0.36:1.00<sub>EDC/NHS</sub> ink obtained with the 3D-printer (A) Just after printing (B) After gelation by pH (nebulization) and temperature. Representative pictures showing their integrity and manipulability (C) One curve resulted from compression DMA mechanical analysis.

#### 4. Cytotoxicity

Direct and indirect cytotoxicity of the col:chi 0.36:1.00<sub>EDC/NHS</sub> scaffolds were evaluated according to the international standard ISO10993-5 for biomedical devices. In the direct assay, no alterations in cell morphology were observed, indicating null toxic effect. Monolayers cultivated for 24 hours in direct contact with the substrates are shown in Fig. 8, in comparison with controls. In the indirect cytotoxicity test, the exudate of the construct immersion in culture medium, did not affect the cells, which showed normal morphology, both in pure extracts and 1/16 dilution.

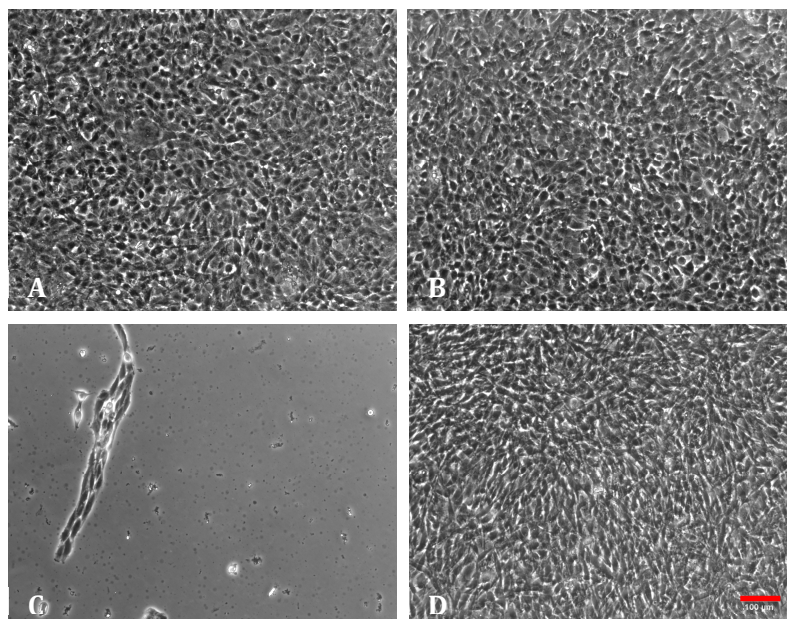


**Figure 8.** NIH/3T3 fibroblasts monolayers after direct cytotoxicity assay. (A) Null control (culture medium). (B) Negative control (Teflon®). (C) Positive control (Latex®). (D) Hydrogel constructs made of col:chi 0.36:1 crosslinked with EDC/NHS. Magnification 100x. Scale bar 100 µm.

## 5. Degradation of scaffolds in PBS and PBS/collagenase

Substrates obtained in 3. from the ink 0.36:1.00<sub>EDC/NHS</sub> were subjected to stability tests at 37 °C in PBS. Fig. 9 shows three curves data: on the first one, % Residual Mass after immersion in PBS at 37 °C (squares), in the second one, a similar protocol but PBS containing physiological collagenase was used for the incubation (circles). By last, constructs made by the same crosslinking method but with collagen only, were used as comparison and as positive control of enzymatic activity (triangles).

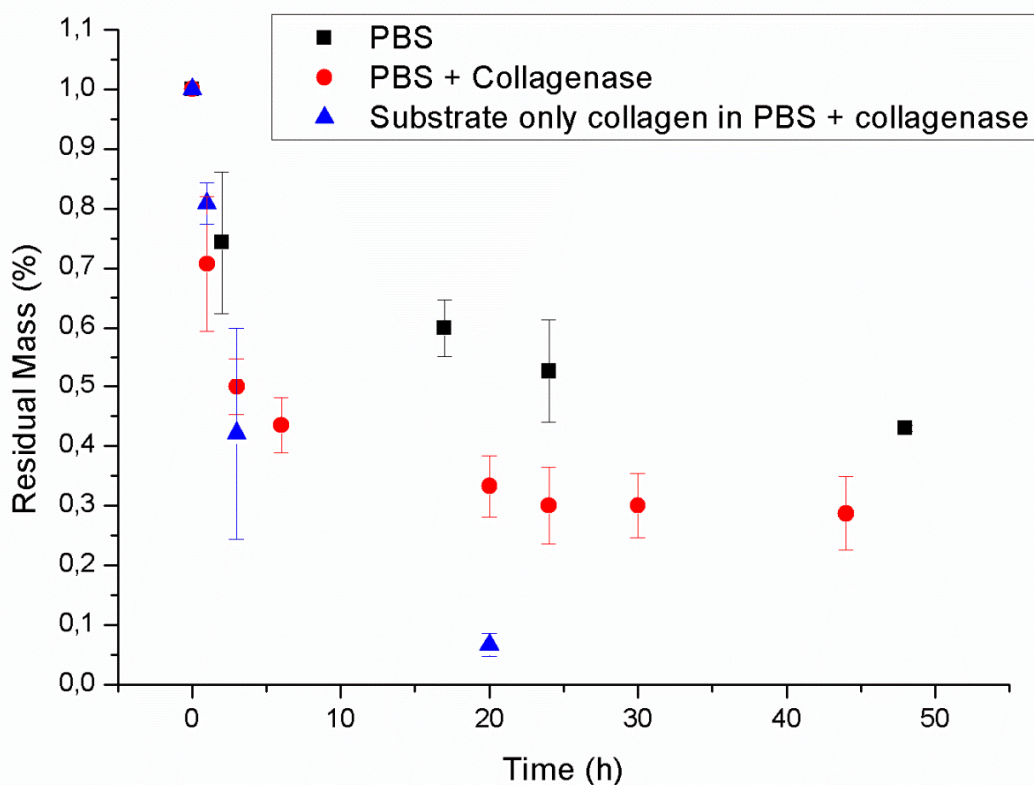


**Figure 9.** Degradation kinetics (% residual mass, % R. M.) for 5 **col:chi 0.36:1<sub>EDC/NHS</sub>** constructs in PBS (black points, squares) and in PBS/collagenase (red points, circles). Collagen substrate, also crosslinked with EDC/NHS, was used as positive control (blue points, triangles). Data represent the average and standard error of 5 determinations.

Mass loss after 48 h in PBS was important, more than 50 %, considering possible uses for tissue engineering. Even with this mass reduction, constructs were perfectly tractable, having kept their integrity. Depending on cell type to be seeded, this feature could be improved by other crosslinking methods or by changing polymer concentrations. We could confirm that most of the loss mass corresponded to water mass, according to a low-viscous hydrogel. By scaffolds freeze-dry before and after incubation determined mass was quite unchanged, being almost all polymer mass, taking into account possible inclusion of PBS salts.

When the PBS curve is compared with PBS+collagenase, the enzyme effect was evident but moderate, considering the % M.R. at 45 h, with also integral and manipulable substrates. In this sense, the collagen construct was fully degraded in 20 h, evidencing the beneficial chitosan content in the selected ratio col:chi 0.36:1.00.

## Conclusions

Taking advantage of the chitosan and collagen proven properties as biomaterials, in this work inks for 3D-bioprinting made of both biopolymers were assessed. Hydrogel precursors were evaluated by rheology, exhibiting low viscosities ( $\eta_{app}$ = 0.35-2.80 Pa.s) and shear-thinning behavior.

The extrusion process in the 3D-bioprinter was evaluated both by printability and rheology. For three inks with different polymer ratios (col:chi 0.18:1.50; col:chi 0.36:1.00 and col:chi 0.54:0.50), acceptable Pr values were found under printing flows between 0.19 uL/s and 0.42 uL/s.

Col:chi 0.36:1.00 was selected in this study and evaluated as a biomaterial for 3D constructs for tissue engineering. The possibility of printing with NHS/EDC into the ink was a suitable way of improving the final construct mechanical properties. Other ways should be explored in this sense, taking into account that keeping on ice the mix as a condition to minimize the viscosity increase is also time-dependent.

Regarding the acidic pH, an apparent drawback due to the solubility of both precursors, a final construct at neutral pH by nebulization was achieved, obtaining mono-layered scaffolds suitable for cell seeding. The main goal of this work was to assess Col-Chi formulations seeking proper rheological properties and printability; the best formulation —col:chi 0.36:1.00— was used to print mono-layered scaffolds. Thinking of multi-layered scaffolds, nebulization *in situ* just after printing might be an alternative.

From these results, other blends partially assessed here, such as col:chi 0.45:1.50 or 0.54:0.50, should be considered for further evaluation. In the same way, alternative crosslinking methods for the selected ink col:chi 0.36:1.00 could be assayed in order to obtain different modulus E for applications in tissue engineering. In addition, more stability at physiological conditions and higher Pr values may be inquired.

We consider the results encouraging, taking into account the innovative 3D-bioprinting technique and the extensive knowledge of collagen and chitosan as biomaterials. Since concentrated materials would provide a restrictive environment for cells, these low concentrated inks show a perspective, using pre-crosslinker modulation to achieve higher printability and finally suitable hydrogel scaffolds.

Declarations of interest: none.

Acknowledgements: FAN (Nanotechnology Argentinian Foundation) and Mr Bernardo Villares and Ms. Camila Ruiz for the AFM images. LIFE-SI and its developer Adén Díaz Nocera because of his constant support with the 3D-bioprinter.

Funding: This work was supported by the Argentinian Ministry of Education through its Secretary of University Policies (grant *Agregando Valor*, Project: Bioinks). A.C.H. was a Biomedical Engineering student with a fellowship of the National Interuniversity Council. M.P.R. was a postdoctoral fellow of CONICET. A.G.W. and E.B.H. are CONICET researchers.

## References

- [1] J. Si, Y. Yang, X. Xing, F. Yang, P. Shan, Controlled degradable chitosan/collagen composite scaffolds for application in nerve tissue regeneration, *Polym. Degrad. Stab.* 166 (2019) 73 - 85. doi:10.1016/j.polymdegradstab.2019.05.023.
- [2] L.A. Reis, L.L.Y. Chiu, Y. Liang, K. Hyunh, A. Momen, M. Radisic, A peptide-modified chitosan-collagen hydrogel for cardiac cell culture and delivery, *Acta Biomater.* 8 (2012) 1022–1036. doi:10.1016/j.actbio.2011.11.030.
- [3] C.D.F. Moreira, S.M. Carvalho, H.S. Mansur, M.M. Pereira, Thermogelling chitosan-collagen-bioactive glass nanoparticle hybrids as potential injectable systems for tissue engineering, *Mater. Sci. Eng. C.* 58 (2016) 1207–1216. doi:10.1016/j.msec.2015.09.075.
- [4] P. Deb, A.B. Deoghare, A. Borah, E. Barua, S. Das Lala, Scaffold Development Using Biomaterials: A Review, *Mater. Today Proc.* 5 (2018) 12909–12919. doi:10.1016/j.matpr.2018.02.276.
- [5] W. L. Ng, C.K. Chua, Y.F. Shen. Print Me An Organ! Why We Are Not There Yet. *Progress in Polym. Sci.* 97 (2019) 101145.
- [6] W.L. Ng, S. Wang, W.Y. Yeong, M.W. Naing, Skin Bioprinting: Impending Reality or Fantasy?, *Trends Biotechnol.* 34 (2016) 689–699. doi:10.1016/j.tibtech.2016.04.006.
- [7] J.K. Carrow, P. Kerativitayanan, M.K. Jaiswal, G. Lokhande, A.K. Gaharwar, *Polymers for bioprinting, Essentials 3D Biofabrication Transl.* (2015) 229–248. doi:10.1016/B978-0-12-800972-7.00013-X.
- [8] J. Malda, J. Visser, F.P. Melchels, T. Jüngst, W.E. Hennink, W.J.A. Dhert, J. Groll, D.W. Huttmacher, 25th Anniversary Article : Engineering Hydrogels for Biofabrication, (2013) 1–18. doi:10.1002/adma.201302042.
- [9] B. Duan, L.A. Hockaday, K.H. Kang, J.T. Butcher, 3D Bioprinting of heterogeneous aortic valve conduits with alginate/gelatin hydrogels, *J. Biomed. Mater. Res. - Part A.* 101 A (2013) 1255–1264. doi:10.1002/jbm.a.34420.
- [10] R. Gaetani, P.A. Doevendans, C.H.G. Metz, J. Alblas, E. Messina, A. Giacomello, J.P.G. Sluijter, Cardiac tissue engineering using tissue printing technology and human cardiac progenitor cells, *Biomaterials.* 33 (2012) 1782–1790. doi:10.1016/j.biomaterials.2011.11.003.
- [11] Y. Yan, X. Wang, Y. Pan, H. Liu, J. Cheng, Fabrication of viable tissue-engineered constructs with 3D cell-assembly technique, *26* (2005) 5864–5871. doi:10.1016/j.biomaterials.2005.02.027.
- [12] S. Ilkhanizadeh, A.I. Teixeira, O. Hermanson, Inkjet printing of macromolecules on hydrogels to steer neural stem cell differentiation, *Biomaterials.* 28 (2007) 3936–3943. doi:10.1016/j.biomaterials.2007.05.018
- [13] A.A.S. Machado, V.C.A. Martins, A.M.G. Plepis, Thermal and rheological behavior of collagen: Chitosan blends, *J. Therm. Anal. Calorim.* 67 (2002) 491–498. doi:10.1023/A:1013953316829.
- [14] Y. He, F. Yang, H. Zhao, Q. Gao, B. Xia, J. Fu, Research on the printability of hydrogels in 3D bioprinting, *Sci.*

- 506 Rep. 6 (2016) 1–13. doi:10.1038/srep29977.
- 507 [15] L. Ouyang, R. Yao, Y. Zhao, W. Sun, Effect of bioink properties on printability and cell viability for 3D  
508 bioplotting of embryonic stem cells, *Biofabrication*. 8 (2016). doi:10.1088/1758-5090/8/3/035020.
- 509 [16] L.P. Yan, Y.J. Wang, L. Ren, G. Wu, S.G. Caridade, J.B. Fan, L.Y. Wang, P.H. Ji, J.M. Oliveira, J.T. Oliveira,  
510 J.F. Mano, R.L. Reis, Genipin-cross-linked collagen/chitosan biomimetic scaffolds for articular cartilage tissue  
511 engineering applications, *J. Biomed. Mater. Res. - Part A*. 95 A (2010) 465–475. doi:10.1002/jbm.a.32869.
- 512 [17] L. Bi, Z. Cao, Y. Hu, Y. Song, L. Yu, B. Yang, J. Mu, Z. Huang, Y. Han, Effects of different cross-linking  
513 conditions on the properties of genipin-cross-linked chitosan/collagen scaffolds for cartilage tissue engineering, *J. Mater.*  
514 *Sci. Mater. Med.* 22 (2011) 51–62. doi:10.1007/s10856-010-4177-3.
- 515 [18] L. Ma, C. Gao, Z. Mao, J. Zhou, J. Shen, X. Hu, C. Han, Collagen/chitosan porous scaffolds with improved  
516 biostability for skin tissue engineering, *Biomaterials*. 24 (2003) 4833–4841. doi:10.1016/S0142-9612(03)00374-0.
- 517 [19] V.A. Reyna-Urrutia, V. Mata-Haro, J. V. Cauich-Rodriguez, W.A. Herrera-Kao, J.M. Cervantes-Uc, Effect of two  
518 crosslinking methods on the physicochemical and biological properties of the collagen-chitosan scaffolds, *Eur. Polym. J.*  
519 117 (2019) 424–433. doi:10.1016/j.eurpolymj.2019.05.010.
- 520 [20] A. Martínez, M.D. Blanco, N. Davidenko, R.E. Cameron, Tailoring chitosan/collagen scaffolds for tissue  
521 engineering: Effect of composition and different crosslinking agents on scaffold properties, *Carbohydr. Polym.* (2015).  
522 doi:10.1016/j.carbpol.2015.06.084.
- 523 [21] D. Wang, M. Wang, A. Wang, J. Li, X. Li, H. Jian, S. Bai, J. Yin, Preparation of collagen/chitosan microspheres  
524 for 3D macrophage proliferation in vitro, *Colloids Surfaces A Physicochem. Eng. Asp.* 572 (2019) 266–273.  
525 doi:10.1016/j.colsurfa.2019.04.007.
- 526 [22] K. Lewandowska, A. Sionkowska, S. Grabska, B. Kaczmarek, M. Michalska, The miscibility of  
527 collagen/hyaluronic acid/chitosan blends investigated in dilute solutions and solids, *J. Mol. Liq.* 220 (2016) 726–730.  
528 doi:10.1016/j.molliq.2016.05.009.
- 529 [23] A. Gilarska, J. Lewandowska-Łańcucka, W. Horak, M. Nowakowska, Collagen/chitosan/hyaluronic acid – based  
530 injectable hydrogels for tissue engineering applications – design, physicochemical and biological characterization,  
531 *Colloids Surfaces B Biointerfaces*. 170 (2018) 152–162. doi:10.1016/j.colsurfb.2018.06.004.
- 532 [24] C. Deng, P. Zhang, B. Vulesevic, D. Kuraitis, F. Li, A.F. Yang, M. Griffith, M. Ruel, E.J. Suuronen, A collagen-  
533 chitosan hydrogel for endothelial differentiation and angiogenesis, *Tissue Eng. - Part A*. 16 (2010) 3099–3109.  
534 doi:10.1089/ten.tea.2009.0504.
- 535 [25] S. V. Murphy, A. Skardal, A. Atala, Evaluation of hydrogels for bio-printing applications, *J. Biomed. Mater. Res. -*  
536 *Part A*. 101 A (2013) 272–284. doi:10.1002/jbm.a.34326.
- 537 [26] J. Habermehl, J. Skopinska, F. Boccafoschi, A. Sionkowska, H. Kaczmarek, G. Laroche, D. Mantovani,  
538 Preparation of ready-to-use, stockable and reconstituted collagen, *Macromol. Biosci.* 5 (2005) 821–828.  
539 doi:10.1002/mabi.200500102.
- 540 [27] N. Rajan, J. Habermehl, M.F. Coté, C.J. Doillon, D. Mantovani, Preparation of ready-to-use, storable and  
541 reconstituted type I collagen from rat tail tendon for tissue engineering applications, *Nat. Protoc.* 1 (2007) 2753–2758.  
542 doi:10.1038/nprot.2006.430.
- 543 [28] M.H. Amer, F.R.A.J. Rose, K.M. Shakesheff, M. Mado, L.J. White, Translational considerations in injectable cell-  
544 based therapeutics for neurological applications: concepts, progress and challenges, *Npj Regen. Med.* 2 (2017).



doi:10.1038/s41536-017-0028-x.

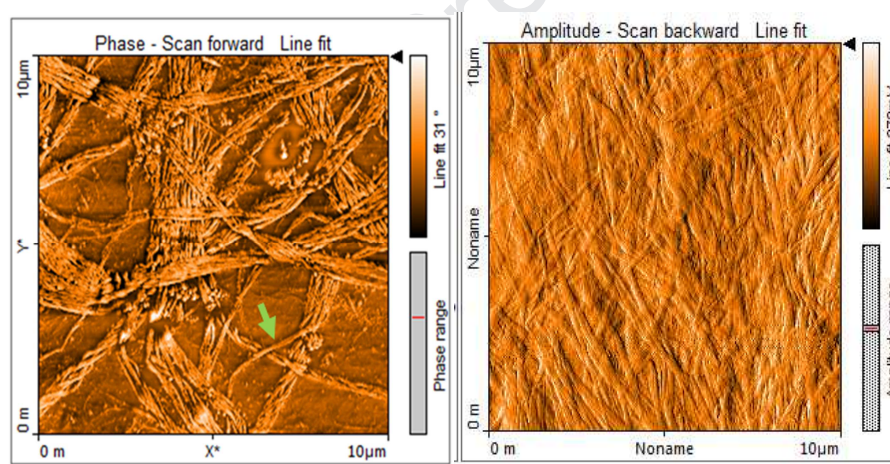
[29] N. Paxton, W. Smolan, T. Böck, F. Melchels, J. Groll, T. Jungst, Proposal to assess printability of bioinks for extrusion-based bioprinting and evaluation of rheological properties governing bioprintability, *Biofabrication* 9 (2017). doi:10.1088/1758-5090/aa8dd8.

[30] J.M. Townsend, E.C. Beck, S.H. Gehrke, C.J. Berkland, M.S. Detamore, Flow behavior prior to crosslinking: The need for precursor rheology for placement of hydrogels in medical applications and for 3D bioprinting, *Prog. Polym. Sci.* (2019). doi:10.1016/j.progpolymsci.2019.01.003.

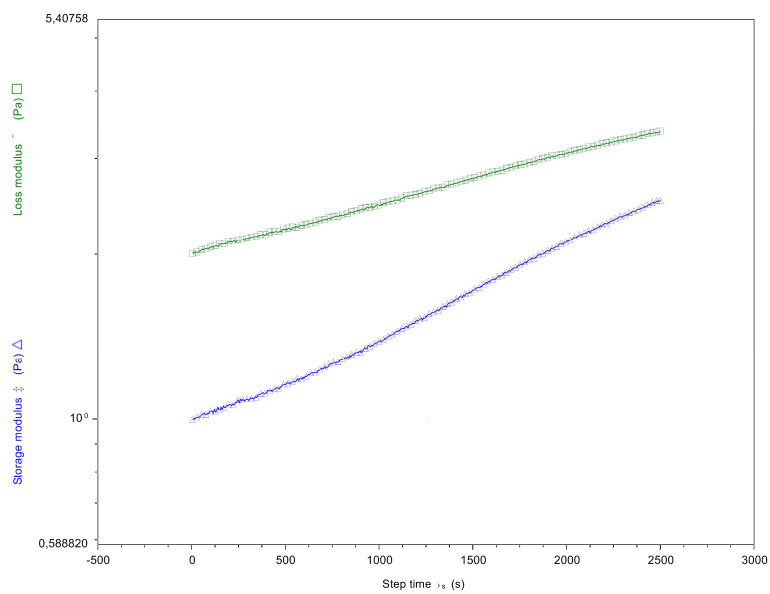
[31] F. Pati, J. Jang, J.W. Lee, D.W. Cho, Extrusion bioprinting, *Essentials 3D Biofabrication Transl.* (2015) 123–152. doi:10.1016/B978-0-12-800972-7.00007-4.

[32] M.M. Laronda, A.L. Rutz, S. Xiao, K.A. Whelan, F.E. Duncan, E.W. Roth, T.K. Woodruff, R.N. Shah, A bioprosthetic ovary created using 3D printed microporous scaffolds restores ovarian function in sterilized mice, *Nat. Commun.* 8 (2017) 1–10. doi:10.1038/ncomms15261.

## Supplementary Data



**Supplementary Data Fig. 1:** Collagen fibrils obtained from rat tail by extraction in acetic acid, observed by AFM images. In addition to the morphological observation, diameter sizes were calculated from the image, comparing with those reported for collagen fibrils in literature, 90 - 120 nm. Green arrow shows a representative 100 nm width fibril.



570

571

572

**Supplementary Data Fig. 2:** Time sweep at 0°C to col:chi 0.36:1.00<sub>NHS/EDC</sub>. Until 2500 seconds no gelation was observed.

- 3D-bioprinting is a powerful emerging field in which ink composition is a critical issue.
- Collagen and chitosan are very well-known biopolymers.
- Blends of collagen and chitosan composing a bioink are poorly explored.
- Collagen and chitosan blends behavior through a 3D-bioprinter were assessed in this work.
- Printed and crosslinked scaffolds for tissue engineering were obtained from col:chi 0.36:1.00, both % w/v.

Journal Pre-proof

Author Statement

Ana Carolina Heidenreich: Conceptualization, Methodology, Investigation, Visualization, Writing – Original Draft.

Mercedes Pérez-Recalde: Conceptualization, Methodology, Writing - Original Draft, Writing - review and Editing, Project Administration.

Ana Gonzalez Wusener: Methodology, Investigation.

Elida Beatriz Hermida: Funding Acquisition, Project Administration, Supervision, Resources.

Journal Pre-proof

Buenos Aires, December 6th 2019

Polymer Testing

Associate Editor Dong Qiu

The authors of the current manuscript "Collagen and Chitosan blends for 3D-bioprinting: a rheological and printability approach" declare not to have conflict of interests about this subject. It contains just a scientific work at our National University of San Martin, Argentina.

Yours sincerely,



Mercedes Pérez-Recalde

Corresponding Author

Journal Pre-proof